

Optimizing turbine location in upgraded wind farm using grasshopper optimization algorithm

Khoa Dang Nguyen^{1,2}, Tinh Trung Tran², Dieu Ngoc Vo^{1,3}

¹Department of Power Systems, Faculty of Electrical and Electronics Engineering, Ho Chi Minh City University of Technology (HCMUT), Ho Chi Minh City, Vietnam

²College of Engineering Technology, Can Tho University, Cần Thơ, Vietnam

³Vietnam National University Ho Chi Minh City, Linh Trung Ward, Thu Duc City, Ho Chi Minh City, Vietnam

Article Info

Article history:

Received Jun 18, 2024

Revised Oct 30, 2024

Accepted Nov 19, 2024

Keywords:

Annual energy production

Grasshopper optimization algorithm

Optimization algorithm

Wake effect

Wind farm layout

windPRO software

ABSTRACT

This research explores the use of the grasshopper optimization algorithm (GOA) for optimizing the placement of additional turbines in an established wind farm. The primary objective is to increase the annual energy production (AEP) of the wind farm while minimizing the wake effects caused by both existing and new turbines. The research evaluates three different turbine types (1.5 MW, 2.0 MW, and 2.5 MW) to identify the most appropriate choice for increasing the wind farm's capacity. The GOA's performance is compared with the commercial software windPRO and validated using WAsP software for energy calculations. Numerical results indicate that the GOA effectively improves wind farm layout, with the 1.5 MW turbines identified as the optimal choice for maximizing AEP and minimizing wake interactions. This study provides practical insights for wind farm operators and contributes to the development of advanced optimization techniques in wind energy.

This is an open access article under the [CC BY-SA](#) license.



Corresponding Author:

Dieu Ngoc Vo

Faculty of Electrical and Electronics Engineering, Ho Chi Minh City University of Technology (HCMUT)
268 Ly Thuong Kiet Street, District 10, Ho Chi Minh City, Vietnam

Email: vndieu@hcmut.edu.vn

1. INTRODUCTION

The global effort to mitigate climate change has put renewable energy at the forefront of environmental initiatives. As nations seek to curtail greenhouse gas emissions, various sustainable power sources have gained prominence. Among these, wind energy has emerged as a particularly promising option, offering significant potential for eco-friendly electricity generation. This growing sector has attracted attention from researchers and policymakers alike, who recognize its capacity to contribute substantially to a cleaner energy landscape [1], [2]. However, optimizing wind farm layouts remains a significant challenge due to the complex interactions between turbines and the variability of wind conditions.

Wind farm design optimization plays a crucial role in enhancing energy output while reducing expenses. A significant hurdle in this process is addressing the wake phenomenon, where turbines positioned downwind experience diminished wind velocities and heightened turbulence due to the influence of upwind turbines. This phenomenon, called the wake effect, is a significant factor in wind farm layout optimization (WFLO). It can greatly impact the overall productivity and efficiency of the wind farm [3], [4]. The optimization of turbine placement in wind farms has been the focus of numerous research studies. Mosetti *et al.* [5] pioneered the use of Jensen's [6] wake model in conjunction with a genetic algorithm (GA) for this purpose, while Yang *et al.* [7] classified WFLO literature and conducted multi-objective optimization. To enhance financial analysis methods for wind farm projects, researchers such as Marmidis *et al.* [8] utilized

probabilistic modeling techniques, specifically implementing Monte Carlo simulations in their work. Şişbot *et al.* [9] optimized layouts on Gökçeada Island with a multi-objective GA. Wan *et al.* [10] found particle swarm optimization (PSO) more effective than GA for maximizing annual energy production (AEP). Kusiak and Song [11] used an evolutionary strategy to optimize AEP and minimize constraints. Saavedra-Moreno *et al.* [12] proposed a new evolutionary algorithm considering various factors and used a greedy heuristic for initialization. Archer *et al.* [13] developed a wake effects coefficient for mixed integer linear programming. Intelligent methods have been effectively used in various wind farm optimization challenges [14]. Meta-heuristic algorithms, drawing inspiration from biological behaviors, have demonstrated impressive performance in tackling complex problems and are extensively used in real-world applications [15]–[20]. Prominent examples include GA, PSO [21], [22], gravitational search algorithm (GSA), and differential evolution (DE) [23], grey wolf optimizer (GWO) and whale optimization algorithm (WOA) [24], [25]. As an alternative approach, these algorithms also perform well in WFLO tasks, with GA being particularly prevalent [26].

Although GAs are widely used, they often struggle with issues like low performance and getting trapped in local optima. To address these limitations, new algorithms have been developed. For example, Beşkirli *et al.* [27] introduced a binary artificial algae algorithm, while Eroğlu and Seçkiner [28] implemented an ant colony optimization (ACO) algorithm with an innovative pheromone update method. Additional approaches include the elephant herding optimization algorithm [29], PSO for offshore wind farms [30], and the use of neural networks as surrogate models [31]. Ju *et al.* [32] combined GA with support vector regression to identify and replace underperforming turbines, leading to improved overall farm efficiency. In a separate investigation, Bai *et al.* [33] augmented GA by incorporating Monte Carlo tree search methods, which enhanced the algorithm's ability to explore potential solutions. These investigations highlight the promise of advanced computational approaches in refining wind farm layouts. Nevertheless, the field continues to seek more powerful and streamlined optimization strategies to further improve wind farm design and performance.

The grasshopper optimization algorithm (GOA) is a relatively new nature-inspired optimization technique [34]–[36]. Modeled after the swarming behavior of grasshoppers, GOA has demonstrated its potential in addressing complex optimization challenges by efficiently balancing exploration and exploitation. This research aims to utilize the GOA to optimize the placement of additional turbines in an existing wind farm, taking into account wake effects and the influence of different turbine types on AEP.

The studies mentioned above demonstrate the strong performance of meta-heuristic algorithms in WFLO, particularly for new wind farms and under simple wind scenarios. However, only a few have explored their effectiveness in complex wind scenarios or in upgrading existing wind farms. For example, Abdulrahman and Wood [37] proposed a method to enhance wind farm layouts by introducing different commercial turbines into an existing farm, using GA for optimization. As the demand for renewable energy grows, upgrading existing wind farms by adding more turbines has become an increasingly practical approach to increasing energy production. This research explores the optimization of existing wind farm expansions, an area often overlooked in current literature. We examine how to best integrate new turbines into operational farms, considering both the interactions between new and existing turbines and the farm's overall performance. This approach aims to maximize energy output in upgraded wind facilities.

The contributions of this study are threefold:

- a. Implement the GOA to determine ideal locations for new turbines within an operational wind farm, showcasing the algorithm's capability in this novel application.
- b. Evaluate the performance of different turbine types (1.5 MW, 2.0 MW, and 2.5 MW) in the optimization process, providing insights into the most suitable turbine type for upgrading wind farms.
- c. Validate the proposed optimization method using WAsP [38] software for energy calculations and compare the results with those obtained from the commercial windPRO software [39].

This article is organized into the following sections: section 2 details wind farm modeling, covering key assumptions, wake effect analysis, and wind power calculation methods. Section 3 introduces the GOA and explains its application to WFLO. Section 4 presents our numerical experiment results, comparing various turbine types and contrasting the proposed algorithm's performance against commercial software solutions. Section 5 presents the conclusions, highlighting the main outcomes of investigation and suggesting potential directions for subsequent studies.

2. WIND FARM MODELING

2.1. Assumptions

To create a standardized model for optimizing turbine locations in a wind farm, we employ the following premises:

- Uniform turbine specifications: every turbine within the facility is assumed to have identical characteristics and technical specifications.
- Fixed turbine count: the total number of wind turbines (N) is predetermined and remains constant throughout the optimization process.
- Two-dimensional representation: the wind farm is modeled on a flat (x, y) coordinate system, assuming minimal variations in elevation and surface conditions. Each turbine's position is denoted by its coordinates (x_i, y_i) , where i ranges from 1 to the total number of turbines, N .
- Wind speed distribution: the wind speed v , occurring in direction θ across the farm, is characterized using a Weibull probability distribution [40]–[43].

In wind energy research, the Weibull distribution is commonly used to model wind speed patterns because of its effectiveness in representing wind speed probability distributions. This statistical model is characterized by two essential parameters: the scale parameter (c) and the shape parameter (k), which determine the distribution's form and magnitude, respectively. The probability density function of the Weibull distribution is given by (1):

$$f(v, k, c) = \frac{k}{c} \left(\frac{v}{c}\right)^{k-1} e^{-\left(\frac{v}{c}\right)^k} \quad (1)$$

2.2. Wake effect model

The wake produced by a wind turbine can be separated into two regions: the near wake, located just behind the rotor, and the far wake, which extends further beyond this zone. In optimizing wind farm layouts for AEP, the far wake is more critical due to reduced velocity and increased turbulence, which significantly lowers overall output [44]. This effect, caused by upstream turbines, impacts the performance of downstream turbines, making precise wake modeling essential for efficient turbine placement. The impact is even greater in wind farms with multiple turbines, where one turbine's wake can affect several others [44].

Researchers have employed a variety of wake models to illustrate the patterns of wind speed reductions [45], [46]. These models can be broadly categorized into two main groups: analytical and computational. While computational models, which rely on solving the Navier-Stokes equations, typically offer greater precision than other modeling techniques, their extensive computational requirements and associated expenses render them unsuitable for application in WFLO [47].

The wake effect model is crucial in the optimization of wind farm layouts. This model simulates how turbines interact with each other, accounting for the decreased wind velocity and heightened turbulence caused by turbines positioned upstream. A simple tail effect model was introduced based on linear assumptions Jensen, where the reduced wind speed is determined by the distance from the turbine. This model is relatively straightforward, with the authors positing that the linear expansion of the wake effect behind wind turbines is contingent on the downstream distance between turbines, as illustrated in Figure 1 using wake model of Jensen.

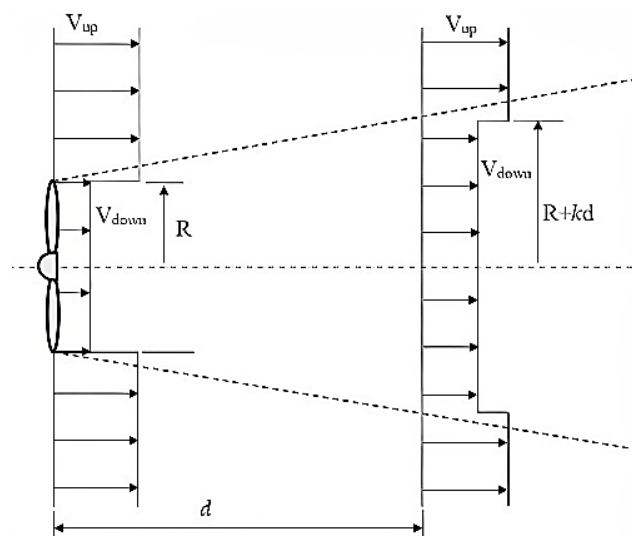


Figure 1. The Jensen's wake model [6]

The fall in wind speed at a certain location d is:

$$V_{def} = 1 - \frac{V_{down}}{V_{up}} = \frac{1 - \sqrt{1 - C_t}}{\left(1 + \frac{\kappa d_{ij}}{R}\right)^2} \quad (2)$$

where, the turbine's thrust coefficient is denoted by C_t , while d_{ij} signifies the projection of the distance between the i^{th} and j^{th} turbines along the wind's direction. The entrainment constant, also known as the decay coefficient, is represented by k and is determined empirically [48], as (3):

$$k = \frac{0.5}{\ln(H/z_0)} \quad (3)$$

where, the hub height is represented by H , while z_0 indicates the terrain's surface roughness. For land-based areas, the constant k is assigned a value of 0.075, whereas for offshore regions, it is set to 0.04. Turbine j^{th} is considered to be within the wake of turbine i^{th} if it lies inside the wake cone, as shown in Figure 2. The distance from turbine i^{th} to turbine j^{th} , projected along the wind direction θ , d_{ij} , is defined as (4) [11]:

$$d_{i,j} = |(x_i - x_j) \cos \theta + (y_i - y_j) \sin \theta| \quad (4)$$

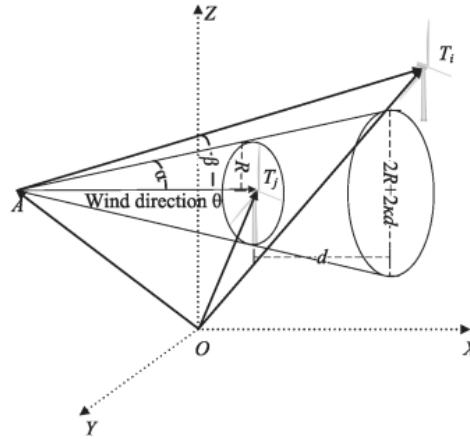


Figure 2. A wind turbine located within the wake cone of another turbine [11]

The wind speed reduces due to the wake effect, which occurs when a turbine is impacted by several turbines situated in front of it.

$$V_{defi} = \sqrt{\sum_{j=1, j \neq i, \beta_{i,j} < \alpha}^N \left[\frac{1 - \sqrt{1 - C_t}}{\left(1 + \kappa d_{i,j}/R\right)^2} \right]} \quad (5)$$

where, parameter $\alpha (0 \leq \alpha \leq \pi/2)$ is defined as $\arctan(\kappa)$ and the angle $\beta_{i,j}$, ($0 \leq \beta \leq \pi$), between the vector originating from the apex of the hypothetical cone to the i^{th} turbine and the j^{th} turbine, is calculated as (6):

$$\beta_{i,j} = \cos^{-1} \left\{ \frac{(x_i - x_j) \cos \theta + (y_i - y_j) \sin \theta + R/\kappa}{\sqrt{\left(x_i - x_j + \frac{R}{\kappa} \cos \theta\right)^2 + \left(y_i - y_j + \frac{R}{\kappa} \sin \theta\right)^2}} \right\} \quad (6)$$

It is clear that the configuration of every turbine and the direction of the wind θ have an impact on V_{defi} . Research has indicated that wake losses affect the Weibull distribution's scaling parameter c alone. According to statistical analysis, the wake effect looks like this [49]:

$$c'(\theta) = c(\theta) \cdot (1 - V_{defi}) \quad (7)$$

2.3. Wind turbine characteristics

Precisely characterizing turbine attributes is essential for accurately predicting wind energy output. Different techniques, such as using approximate polynomials, have been utilized to model wind turbines [50]. In this study, a 9th order polynomial model is employed as it has been found to be appropriate.

$$f(x) = p_0 + p_1x + p_2x^2 + p_3x^3 + p_4x^4 + p_5x^5 + p_6x^6 + p_7x^7 + p_8x^8 + p_9x^9 \quad (8)$$

The standard case is applied to the problem with turbine capacities of 1.5 MW, 2.0 MW, and 2.5 MW as shown in Table 1.

Table 1. Types of turbines proposed for wind farms

Type of turbine		FLMD 1.5 MW	VESTAS 2.0 MW	GE 2.5 MW
General data	Rated power (kW)	1500	2000	2500
	Rotor diameter (m)	77	100	100
	Number of blades	3	3	3
Rotor	Minimum speed (rd/min)	9.7	-	5.0
	Maximum speed (rd/min)	18.3	13.4	14.1
	Cut-in wind speed (m/s)	3.5	3.5	3.0
	Rated wind speed (m/s)	13.5	12	11.5
	Cut-off wind speed (m/s)	20	22	25
Generator	Maximum speed (rd/min)	1800	-	1650
	Voltage (V)	690	-	690

Figure 3 presents the polynomial model, which integrates realistic wind turbine characteristics as proposed in this paper. The results show that the modeled characteristics closely align with those of actual turbines. Specifically, Figure 3(a) depicts the power characteristics of the FLMD-1.5 MW turbine, Figure 3(b) illustrates those of the VESTAS-2.0 MW turbine, and Figure 3(c) represents the GE-2.5 MW turbine.

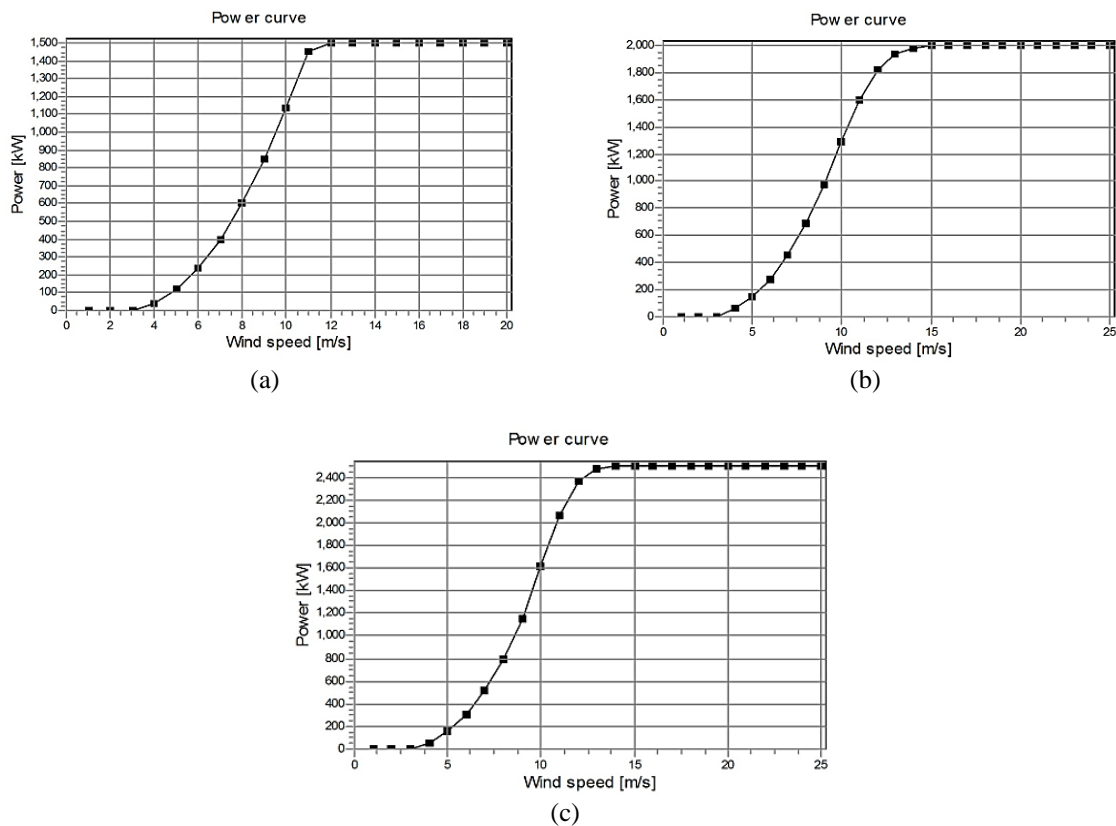


Figure 3. Turbine characteristics; (a) FLMD 1.5 MW turbine characteristic, (b) VESTAS 2.0 MW turbine characteristic, and (c) GE 2.5 MW turbine characteristic

Therefore, the wind turbine characteristics are restated as (9):

$$f(v) = \begin{cases} 0, & v_i < v_{cutin}, v_i > v_{cutout} \\ f(x) \text{ in Eq. (8)}, & v_{cutin} \leq v_i \leq v_{cutout} \\ P_{rated}, & v_{rated} \leq v_i \leq v_{cutout} \end{cases} \quad (9)$$

2.4. Wind power model

2.4.1. Wind model

The wind model is essential for forecasting wind power, as wind speed and direction affect turbine efficiency. Wind speed is typically modeled using a Weibull distribution, while wind direction is analyzed through a wind rose. For wind farm layout design, a 12-sector wind rose is recommended.

2.4.2. Wind power output

By multiplying the power created at each wind speed by the period for which that particular wind speed occurs, and then integrating this across all conceivable wind speeds, one may get the average power produced by a wind turbine. In (10) represents the turbine's energy production [51]:

$$E(P, \theta) = \int_0^\infty f(v) p(v, c(\theta), k(\theta)) dv \quad (10)$$

where, the expression $p(v, c(\theta), k(\theta))$ denotes the Weibull probability density function for wind speed, while $f(v)$ signifies the power curve, as outlined in (9). The computation of energy generated by a turbine for wind directions varying from 0° to 360° is detailed as (11):

$$E(P) = \int_0^{360} p(\theta) d\theta \int_0^\infty f(v) p(v, c(\theta), k(\theta)) dv \quad (11)$$

The energy output of the wind farm will be determined through numerical integration. The overall energy production for each wind direction θ will be aggregated as (12) [11]:

$$E(P) = \sum_{i=1}^h f_i(\theta) \int_0^\infty f(v) \frac{k_i(\theta)}{c_i'(\theta)} \left(\frac{v}{c_i'(\theta)} \right)^{(k_i(\theta)-1)} e^{-\left(\frac{v}{c_i'(\theta)} \right)^{k_i(\theta)}} dv \quad (12)$$

3. METHOD

3.1. Objective function

The process of optimizing turbine location focuses on addressing new challenges, such as integrating advanced turbines with varying specifications, reducing wake losses, and adapting to shifts in wind patterns due to changes in surrounding landscapes. Therefore, properly optimizing turbine locations can significantly increase the AEP, reduce maintenance costs, and improve the overall sustainability of the wind farm. This research presents a strategy to optimize the turbine layout in a wind farm to increase AEP. The objective function for the considered problem is as (13):

$$Obj = \max[\sum E(P)] \quad (13)$$

3.2. Optimization algorithm

The intricate nature of wind farm optimization, coupled with the constraints of trial-and-error techniques, makes heuristic approaches more favorable, as they effectively address these design challenges. For this study, we have selected the GOA to optimize turbine placement during the upgrade of existing wind farms. The GOA is a nature-inspired swarm intelligence method, modeled on the foraging and collective swarming behavior observed in grasshoppers. Widely adopted by researchers, GOA has proven effective in solving various optimization problems. Grasshoppers' unique social interactions and predatory strategies, involving continuous position updates and comfort zone adjustments, enable them to balance global and local search, successfully identifying optimal solutions [34].

The larval phase of grasshopper swarms is characterized by slow, small-step movement. In contrast, the adult swarm exhibits long-range, abrupt movement. Seeking food sources is another key feature of grasshopper swarming behavior. The search process is split into two stages by the GOA, just like other nature-inspired algorithms: exploration and exploitation. In optimization algorithms, two fundamental concepts are exploration and exploitation. Exploration refers to the wide-ranging movement of agents across the search space, while exploitation involves more localized, fine-tuned searches. Interestingly, grasshoppers

in nature display behaviors that mirror these algorithmic concepts. They engage in both broad area searches and focused local movements. Additionally, grasshoppers exhibit a third behavior-the ability to orient themselves towards and move in the direction of specific goals. Modeling this behavior mathematically could enable the design of a new nature-inspired algorithm [34]. Grasshopper swarming behavior can be modeled using the concept of a comfort zone, as illustrated in Figure 4. This social interaction, represented by a function 's', was a key influence on earlier, simplified locust swarm models.

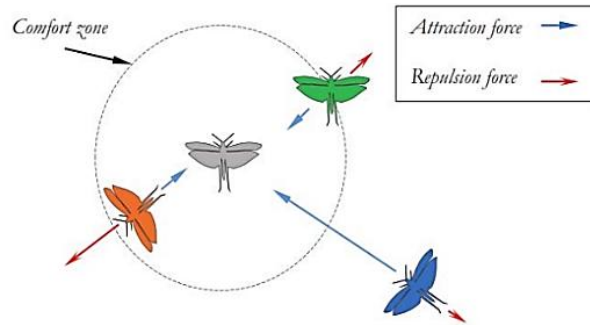


Figure 4. Social interaction of grasshoppers [34]

The mathematical representation of grasshopper swarming behavior can be expressed as (14) [34]:

$$P_i = S_i + G_i + A_i \quad (14)$$

where, P_i represents the location of the i^{th} grasshopper, S_i the social dynamics between grasshoppers in the swarm, G_i indicates the gravitational force acting on the i^{th} grasshopper, and A_i is used to model the effect of wind on grasshopper movement. To incorporate the unpredictable behavior of grasshoppers, may be reformulated as (14):

$$X_i = r_1 S_i + r_2 G_i + r_3 A_i \quad (15)$$

where, r_1 , r_2 , and r_3 are numbers distributed within the range [0, 1]. The definition of social interaction S_i is presented as (16):

$$S_i = \sum_{j=1, j \neq i}^N s(d_{ij}) \hat{d}_{ij} \quad (16)$$

where, d_{ij} is the distance from the i^{th} to the j^{th} grasshopper, calculated as $d_{ij} = |x_j - x_i|$. The function s is used to represent the intensity of social forces; \hat{d}_{ij} is the unit vector pointing from the grasshopper i^{th} to j^{th} , calculated as (17):

$$\hat{d}_{ij} = \frac{x_j - x_i}{d_{ij}} \quad (17)$$

The mathematical representation of social forces among grasshoppers, denoted by the function s , is computed as (18):

$$s(r) = f e^{\frac{-r}{l}} - e^{-r} \quad (18)$$

where, the variable f signifies the intensity of attraction, whereas l indicates the extent of the attractive range. The social dynamics among grasshoppers can be described by forces of attraction and repulsion. These forces are influenced by the distance between the grasshoppers, which is considered within the range of [0, 15]. Attraction intensifies when the distance lies between 2.079 and 4, after which it gradually diminishes. Repulsion, on the other hand, takes place when the distance falls within the range of 0 to 2.079. At an exact distance of 2.079, there is no force acting between the grasshoppers, neither repulsion nor attraction, and this is referred to as the comfort zone [35].

The gravitational force G_i is calculated as (19):

$$G_i = -g\hat{e}_g \quad (19)$$

where, the variable g represents the gravitational constant, and \hat{e}_g denotes the unit vector directed toward the Earth's center.

In (20) shows the wind advection A_i :

$$A_i = u\hat{e}_w \quad (20)$$

where, the drift constant is u and unit vector in the direction of the wind is \hat{e}_w .

By replacing the values of S , G , and A , the resulting equation becomes:

$$X_i = \sum_{j=1, j \neq i}^N s(|x_j - x_i|) \frac{x_j - x_i}{d_{ij}} - g\hat{e}_g + u\hat{e}_w \quad (21)$$

where, the total number of locusts in the population is N .

In (21), cannot be directly applied to optimization tasks due to a specific limitation. In this formulation, the grasshoppers rapidly attain their comfort zone, which results in the swarm's inability to effectively converge on the desired target point [36]. To address this issue, researchers have developed an enhanced version of the equation, which is presented in (22):

$$X_i^d = c \left(\sum_{j=1, j \neq i}^N c \frac{ub_d - lb_d}{2} s(|x_j^d - x_i^d|) \frac{x_j^d - x_i^d}{d_{ij}} \right) + \hat{T}_d \quad (22)$$

where, the terms ub_d and lb_d indicate the upper and lower limits in the d^{th} dimension, respectively. \hat{T}_d signifies the optimal solution found to date within the d^{th} dimensional space.

It's worth noting that S is akin to the S component in (14), the gravitational force component (G) equals zero, and the wind direction component (A) always points towards the best solution \hat{T}_d .

In (22) indicates that a grasshopper's subsequent location is determined by three key factors: its present position, the target location, and the positions of fellow grasshoppers. The equation's first term takes into account the grasshopper's proximity to its peers, which helps ensure that the search agents are distributed around the intended target. The adaptive parameter c appears twice in this equation, serving distinct purposes:

- The initial coefficient c on the left is similar to the inertial weight (w) in PSO. It moderates the grasshoppers' movements toward the target, effectively balancing the exploration and exploitation activities of the entire swarm in relation to the target.
- The second c reduces the areas of attraction, comfort, and repulsion among grasshoppers. In terms of composition $c \frac{ub_d - lb_d}{2} s(|x_j^d - x_i^d|)$, the $c \frac{ub_d - lb_d}{2}$ component plays a role in diminishing the space a locust explores and exploits in a linear fashion, while the $s(|x_j^d - x_i^d|)$ component dictates whether the locust should move away from (explore) or towards (exploit) the target.

$$C = C_{max} - t \frac{C_{max} - C_{min}}{t_{max}} \quad (23)$$

where, t represents the current iteration; and t_{max} is the total number of iterations. A large value of c results in greater exploration in GOA, while a small value of c leads to increased exploitation. The value of c is always set between C_{max} and C_{min} .

In this optimization approach, the position of each grasshopper is adjusted by considering three essential elements: its present coordinates, the optimal position found within the entire swarm, and the positions of its neighboring grasshoppers. This updating strategy helps the algorithm avoid getting trapped in local optimal solutions. The step-by-step process of this optimization technique is outlined in a pseudocode format, which can be found in the first algorithm description [34]. The flowchart illustrating the GOA algorithm is presented in Figure 5.

Algorithm 1. The pseudo-code of the GOA [35]

```

1: Initializing the grasshopper population:  $X_i$  ( $i = 1, 2, \dots, N$ )
2: Setting up algorithm parameters:  $C_{min}$ ,  $C_{max}$ , and  $t_{max}$ 
3: Evaluating initial fitness:  $f(X_i)$  of each  $X_i$ 
4:  $t =$  the best solution
5: while ( $t < t_{max}$ ) do
```



```

6:      Updating the adaptive parameter using Eq. (23)
7:      for i = 1 to N do
8:      Updating grasshopper positions using Eq. (22)
9:      Enforcing search boundaries
10:     end for
11:     Re-evaluating fitness and updating the best solution
12:     t = t + 1
13: end while
14: Returning the best solution found

```

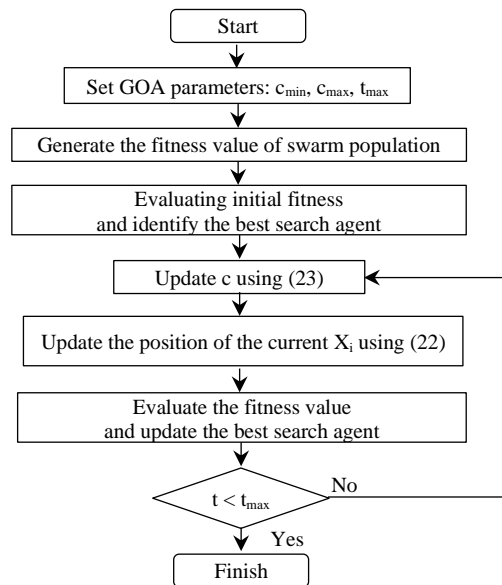


Figure 5. The flowchart of the GOA [35]

Wind farm data plays a vital role in optimizing turbine locations to reduce interference effects and enhance yearly energy output. The wind farm discussed in this paper is an onshore site, derived from the WAsP workspace sample [38], specifically the file Version8Windfarm.wh. This wind farm is situated in a complex terrain with elevations ranging from 10 m to 110.5 m. The site experiences an average wind speed of 7.25 m/s and an average wind energy density of 388 W/m². The goal is to enhance the wind farm configuration for each suggested turbine model to maximize energy output and efficiency, ultimately identifying the most appropriate turbine type.

The task is to increase the output capacity of a current 30 MW wind farm by incorporating an extra 20 MW within the same area, which spans 3000×2500 m². The proposal involves using three types of turbines with different capacities to calculate the total energy output and efficiency of the wind farm in order to select the most suitable turbine type. The parameters of wind farm are shown in Table 2.

Table 2. Input parameters

Parameters	Value
Roughness (Z0)	0.083
Wind velocity in free flow (V0)	7.25 m/s
Hub height (h)	80 m
Existing wind farm area	3000 m×2500 m
Thrust coefficient (Ct)	0.8
Wind density	388 W/m ²

The flow chart of Figure 6 shows the optimization steps applied to optimize an upgraded wind farm [24]. Step 1: raw data of wind, terrain, surface roughness, obstacles, existing turbine locations and wind generator data will be input into WAsP software for processing and the output of this process is the wind resource map. Step 2: the input data for windPRO and GOA is the wind resource map, which will be used to optimally position new turbines within the upgraded wind farm.

Step 3: after the wind farm is optimally arranged by the GOA algorithm, the windPRO software will be recalculated and analyzed by WAsP software.

Step 4: conclusion and proposal of the best solution.

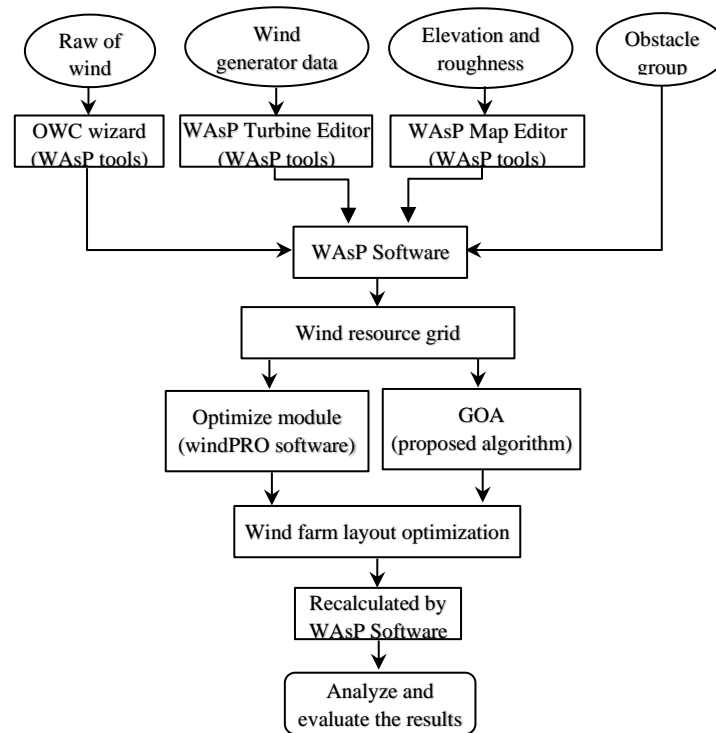


Figure 6. Flow chart of WFLO [24]

4. NUMERICAL RESULTS

The article suggests selecting three different types of wind turbines to be optimally arranged within the same wind farm to assess the algorithm's effectiveness and identify the most suitable turbine type for installation. The case studies are summarized in Table 3. The existing wind farm consists of 20 FMD77 turbines, each with an installed capacity of 1.5 MW, resulting in a total capacity of 30 MW. Detailed data for the current wind farm is presented in Table 4.

Table 3. Case studies of optimization of wind farm layout

Case studies	Case study 1	Case study 2	Case study 3
Turbine capacity [MW]	1.5	2.0	2.5
Number of turbines	14	10	8
Shape of wind farm	Fixed	Fixed	Fixed
vcut-in [m/s]	3.54	3.5	3.5
vcut-out [m/s]	20	22	25

Table 4. Existing wind farm data

Variable	Total	Mean	Min	Max
Gross AEP [GWh]	94.373	4.719	4.511	4.952
Net AEP [GWh]	90.686	4.534	4.359	4.687
Wake loss [%]	3.91	-	0.87	5.35
Mean speed [m/s]	-	7.04	6.9	7.21
Capacity factor [%]	34.508	-	-	-

Table 4 summarizes the data from the existing wind farm, showing that the maximum, minimum, and average Gross AEP per turbine are 4,952 GWh, 4,511 GWh, and 4,719 GWh, respectively. The wind

farm's total Gross AEP, encompassing all 20 turbines, is 94,373 GWh. In terms of Net AEP, the maximum, minimum, and average values per turbine are 4,687 GWh, 4,359 GWh, and 4,534 GWh, respectively, resulting in a total Net AEP of 90,686 GWh. The wake losses for individual turbines vary, with a maximum of 5.35%, a minimum of 0.87%, and an average of 3.91%. The entire wind farm has a capacity factor of 34.508%.

Figure 7 displays the primary wind directions in the project area, with angles of 30, 60, 240, and 270 degrees. The wind roses are simplified and divided into four sectors (sectors 2, 3, 9, and 10) as shown in Figure 7(a). The highest probability was observed at a wind speed of 6.8 m/s, representing approximately 12%, with an average wind power density of 330 W/m², as illustrated in Figure 7(b). Figures 8 and 9 depict the turbine layout and terrain elevation of the existing wind farm, simulated using WAsP software [38].

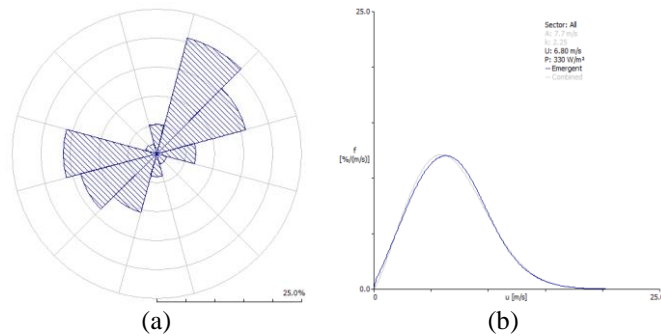


Figure 7. Characteristics of wind energy; (a) wind rose and (b) wind speed distribution

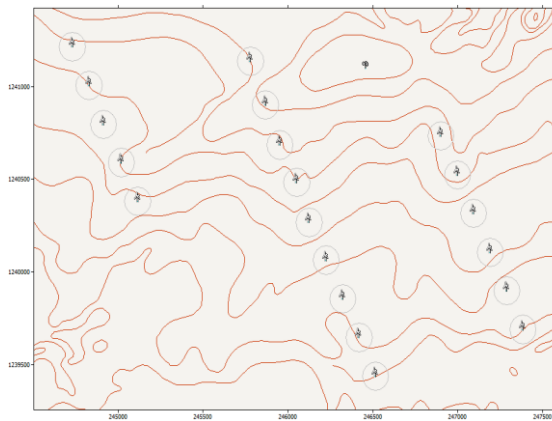


Figure 8. Turbine layout of the existing wind farm using WAsP software

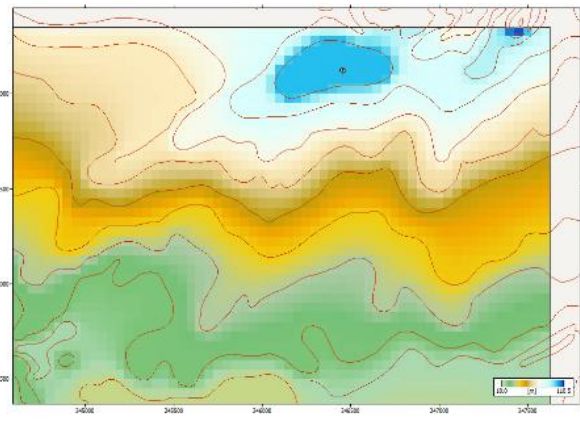


Figure 9. Current wind farm elevation

4.1. Case study 1

In case study 1, it is proposed to utilize 14 FLMD wind turbines, each with a capacity of 1.5 MW, for the upgrade of the existing wind farm. These turbines are strategically positioned in regions with the highest wind energy density and arranged to minimize wake effects, all within the current footprint of the wind farm.

Table 5 presents the calculation results of the GOA algorithm and windPRO software for three scenarios: i) the existing wind farm with 20 turbines considering the wake effect from the additional turbines; ii) 14 additional turbines installed within the existing wind farm area; and iii) the entire upgraded wind farm. Each method produces different calculation results, but both methods show similar efficiency in terms of AEP and wake loss for the existing wind farm, the additional turbines, and the upgraded wind farm.

Table 5. Results of the wind farms using the GOA and windPRO

Variable	GOA			windPRO		
	Existing wind farm	Additional wind farm	Upgraded wind farm	Existing wind farm	Additional wind farm	Upgraded wind farm
Gross AEP [GWh]	94.373	66.186	160.559	94.374	68.927	163.301
Net AEP [GWh]	87.293	59.185	146.478	87.742	62.785	150.527
Wake loss [%]	7.502	10.58	8.77	7.0274	8.91	7.82
Capacity factor [%]	33.217	32.173	32.787	33.387	34.129	33.693

The calculation results show a significant decrease in the wind farm's efficiency after the upgrade, dropping from 34.508% to 32.787% according to GOA, and to 33.693% according to windPRO, following the addition of 14 turbines. The data suggests that increasing the density of wind turbines in a given area leads to more pronounced wake effects. This intensification of wake interference among turbines can result in higher energy losses and a decrease in the overall annual energy output of the wind farm. The wake loss of the wind farm after the upgrade rises significantly from the original 3.91% to 8.77% according to GOA, and to 7.82% according to windPRO. This demonstrates the effectiveness of the GOA algorithm for optimizing wind farm layouts. Each method identified a different layout, but all exhibited similar performance in terms of AEP and wake loss. The wind turbine layout in Figure 10 is closely aligned with the layout shown in windPRO in Figure 11. The additional wind turbines are positioned within the same area as the existing wind farm and are placed in locations with the highest power density. They are optimally arranged to avoid wake effects.

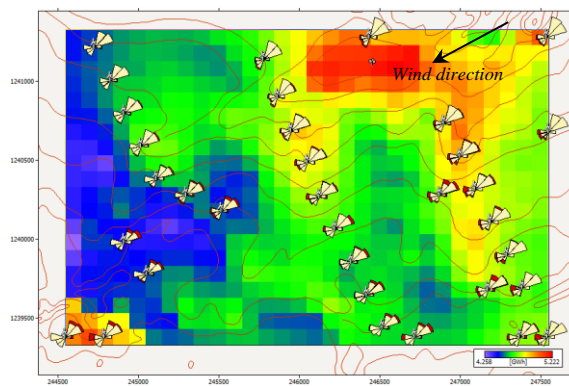


Figure 10. Optimal turbine layout using GOA

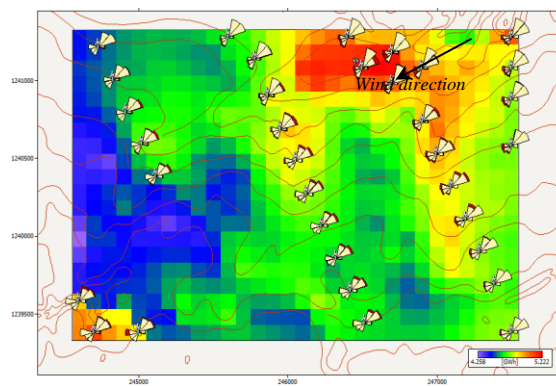


Figure 11. Optimal turbine layout using windPRO

4.2. Case study 2

In this study, 10 VESTAS 2.0 MW wind turbines will be used for optimal layout to upgrade the wind farm. As in case study 1, the GOA algorithm and windPRO software will be applied to evaluate the AEP, wake losses, and efficiency of the newly upgraded turbines, the existing wind farm considering the influence of the additional turbines, and the overall upgraded wind farm.

The calculation results of the GOA algorithm and windPRO software for three scenarios are shown in Table 6. These scenarios include the existing wind farm with 20 turbines considering the wake effect from 10 VESTAS 2.0 MW additional turbines, 10 additional turbines installed within the existing wind farm area, and the entire upgraded wind farm. While the two methods yield different results, they both show similar efficiency in terms of AEP and wake loss for the existing wind farm, the additional turbines, and the upgraded wind farm.

Table 6. Results of the wind farms using the GOA

Variable	GOA			windPRO		
	Existing wind farm	Additional wind farm	Upgraded wind farm	Existing wind farm	Additional wind farm	Upgraded wind farm
Gross AEP [GWh]	94.373	55.269	149.642	94.373	56.015	150.388
Net AEP [GWh]	87.741	50.862	138.603	88.133	52.46	140.593
Wake loss [%]	7.027	7.97	7.38	6.612	6.35	6.51
Capacity factor [%]	33.387	29.031	31.645	33.536	29.943	32.099

The data presented in Table 6 demonstrate a significant reduction in the wind farm's capacity factor post-upgrade. GOA calculations reveal a drop in efficiency from 34.508% to 31.645%, while windPRO shows a decrease to 32.009% with the addition of 10 turbines. This indicates that adding more turbines within the same area amplifies wake effects, leading to greater wake losses and a reduction in energy production. Specifically, wake losses in the wind farm spike from 3.91% to 7.38% according to GOA, and to 6.51% based on windPRO after the upgrade. GOA and windPRO for wind farm layout are different, but all demonstrate similar performance in terms of AEP and wake losses. An examination of Figures 12 and 13 reveals striking similarities between the wind turbine configurations generated by the GOA and the windPRO software, respectively. In both layouts, the newly added turbines are integrated within the existing wind farm's footprint. These additional units appear to be strategically positioned in areas characterized by superior power density. The arrangement suggests a careful optimization process aimed at minimizing wake interference among the turbines.

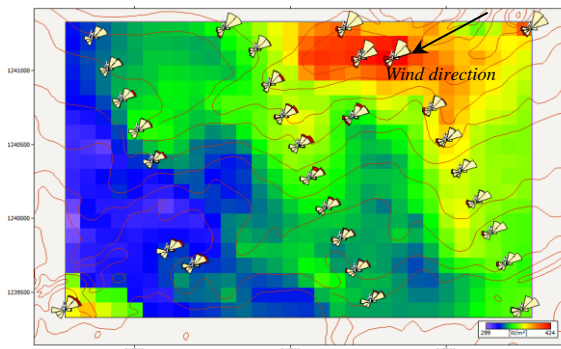


Figure 12. Optimal turbine layout using GOA

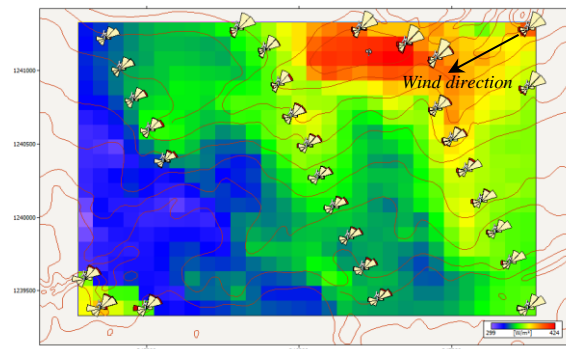


Figure 13. Optimal turbine layout using windPRO

4.3. Case study 3

Expanding on the methodologies employed in the previous two case studies, this investigation proposes the addition of eight GE energy 2.5 MW turbines to enhance the wind farm's capacity. Both the GOA and windPRO software will be utilized to calculate the AEP and wake losses for both the current and expanded wind farm configurations.

The results, summarized in Table 7, indicate a notable reduction in the existing wind farm's AEP following the expansion. The initial net AEP of the current wind farm stands at 90.686 GWh. Post-upgrade simulations show a decrease to 88.759 GWh according to windPRO software, and 88.57 GWh as per the GOA algorithm. This decline in energy output can be attributed to the wake effects introduced by the newly installed turbines, which appear to negatively impact the performance of the existing farm.

Table 7. Results of the wind farms using the GOA

Variable	GOA			windPRO		
	Existing wind farm	Additional wind farm	Upgraded wind farm	Existing wind farm	Additional wind farm	Upgraded wind farm
Gross AEP [GWh]	94.373	55.173	149.546	94.373	57.16	151.533
Net AEP [GWh]	88.57	51.438	140.008	88.759	53.985	142.744
Wake loss [%]	6.15	6.77	6.38	5.949	5.55	5.8
Capacity factor [%]	33.703	29.359	31.966	33.775	30.814	32.589

The data presented in Table 7 demonstrate a significant reduction in the wind farm's capacity factor post-upgrade. GOA calculations reveal a drop in efficiency from 34.508% to 31.966%, while windPRO shows a decrease to 32.589%. This analysis indicates that a higher density of wind turbines within a fixed area intensifies the wake interference phenomenon. As a consequence, there is an observed increase in energy losses due to wake effects, leading to a decrease in the overall energy output of the wind farm. Specifically, wake losses in the wind farm spike from 3.91% to 6.38% according to GOA, and to 5.8% based on windPRO after the upgrade. The results demonstrate a noteworthy decrease in the wind farm's efficiency post-upgrade. Figures 14 and 15 show the turbine layout in the wind farm using GOA and windPRO, respectively. The turbines are arranged similarly in both layouts.

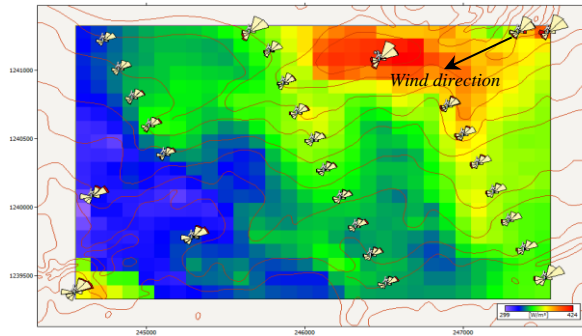


Figure 14. Optimal turbine layout using GOA

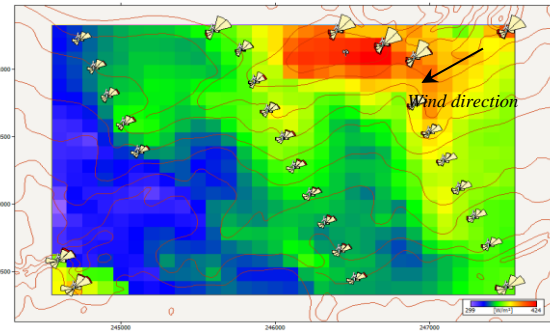


Figure 15. Optimal turbine layout using windPRO

5. DISCUSSION

Optimizing turbine locations in upgraded wind farms is challenging, particularly due to wake effects between existing and new turbines. This study successfully applied the GOA to improve turbine placement and enhance AEP. To evaluate the algorithm's effectiveness, we compared the performance of wind farms optimized by GOA with those calculated by windPRO software, as shown in Table 8.

Table 8. Efficiency of wind farms with optimal turbine placement using windPRO and GOA

Wind farms		Efficiency [%]		
		FLDM 1.5 MW	VESTAS 2.0 MW	GE 2.5 MW
Existing wind farm	windPRO	33.387	33.536	33.774
	GOA	33.217	33.387	33.702
Additional wind farm	windPRO	34.129	29.943	30.813
	GOA	32.173	29.031	29.359
Upgraded wind farm	windPRO	33.693	32.099	32.589
	GOA	32.787	31.645	31.965

The comparison results indicate that the 1.5 MW FLDM turbine is the most efficient for capacity upgrades in the existing wind farm, with an efficiency of 32.787%, outperforming the 2.0 MW VESTAS turbine at 31.645% and the 2.5 MW GE turbine at 31.965%. The relevant data for both the existing wind farm and the newly installed turbines are summarized in Table 8. This result shows that the FLDM 1.5 MW turbine is the most efficient in both the existing and the upgraded wind farm, and GOA has an efficiency close to windPRO in this case.

The GOA results were compared with those from the commercial software windPRO and further validated using WAsP. The comparison shows that GOA offers a robust alternative to traditional methods, delivering notable improvements in AEP. These results underscore the effectiveness of the GOA as a valuable method for enhancing wind farm configurations. The algorithm demonstrates particular utility in scenarios involving the integration of additional turbines into pre-existing wind farm layouts.

Table 9 shows that the Net AEP for the upgraded wind farms calculated using GOA is within 3% of the results from windPRO, demonstrating the algorithm's practicality for wind energy calculations. However, assumptions like constant terrain elevation and surface roughness limit the real-world applicability of this study. Future research should consider more detailed terrain models and compare GOA with other advanced or hybrid algorithms to enhance its performance further.

Table 9. Comparison of Net AEP for upgraded wind farms calculated using windPRO and GOA

Case studies	Variable	Upgraded wind farm	
		windPRO	GOA
Case study 1	Net AEP [GWh]	150.527	146.478
	Comparison (%)	2.690	
Case study 2	Net AEP [GWh]	140.593	138.603
	Comparison (%)	1.415	
Case study 3	Net AEP [GWh]	142.744	140.008
	Comparison (%)	1.917	

In summary, this study demonstrates the GOA's efficacy in refining wind farm configurations. The algorithm provides pragmatic approaches for improving overall wind farm performance, thereby making a significant contribution to the ongoing development of wind energy technologies. The GOA's ability to optimize turbine placement, especially when integrating new units into existing farms, highlights its potential as a valuable tool in the wind energy sector.

6. CONCLUSION

This study highlights the successful application of the GOA in optimizing the placement of additional turbines in a wind farm undergoing upgrades. By effectively accounting for wake effects and analyzing different turbine types, GOA has demonstrated considerable potential in improving the AEP of wind farms.

The use of GOA in this scenario represents a notable advancement over conventional optimization methods. The GOA's balanced approach to exploration and exploitation enables it to effectively search the complex solution landscape, evading local optima and yielding superior optimization results. Validation through comparisons with windPRO and WAsP software reinforces the reliability and accuracy of GOA in practical applications.

The study's analysis of various turbine types (1.5 MW, 2.0 MW, and 2.5 MW) provides important insights for wind farm operators considering upgrades. The 1.5 MW turbines were found to be the most advantageous, offering the best trade-off between energy generation and wake effect reduction. This information is crucial for making well-informed decisions on turbine selection to optimize the efficiency and profitability of wind farm upgrades.

Nonetheless, the study acknowledges certain limitations, such as the assumptions regarding constant terrain elevation and surface roughness. Future research should focus on incorporating more detailed terrain models and varying surface roughness to better reflect real-world conditions. Moreover, further comparisons with other advanced optimization algorithms and the exploration of hybrid methods could yield a deeper understanding of GOA's capabilities and potential areas for improvement.

ACKNOWLEDGMENT

We acknowledge Ho Chi Minh City University of Technology (HCMUT), VNU-HCM for supporting this study.

REFERENCES




- [1] E. T. Sayed *et al.*, "A critical review on environmental impacts of renewable energy systems and mitigation strategies: Wind, hydro, biomass and geothermal," *Science of The Total Environment*, vol. 766, p. 144505, Apr. 2021, doi: 10.1016/j.scitotenv.2020.144505.
- [2] A. G. Olabi and M. A. Abdelkareem, "Renewable energy and climate change," *Renewable and Sustainable Energy Reviews*, vol. 158, p. 112111, Apr. 2022, doi: 10.1016/j.rser.2022.112111.
- [3] R. J. Barthelmie *et al.*, "Modelling and measuring flow and wind turbine wakes in large wind farms offshore," *Wind Energy*, vol. 12, no. 5, pp. 431–444, 2009, doi: 10.1002/we.348.
- [4] K. Xie, H. Yang, B. Hu, and C. Li, "Optimal layout of a wind farm considering multiple wind directions," in *2014 International Conference on Probabilistic Methods Applied to Power Systems (PMAPS)*, Jul. 2014, pp. 1–6, doi: 10.1109/PMAPS.2014.6960594.
- [5] G. Mosetti, C. Poloni, and B. Diviacco, "Optimization of wind turbine positioning in large windfarms by means of a genetic algorithm," *Journal of Wind Engineering and Industrial Aerodynamics*, vol. 51, no. 1, pp. 105–116, Jan. 1994, doi: 10.1016/0167-6105(94)90080-9.
- [6] N. O. Jensen, *A note on wind generator interaction*. Risø National Laboratory: Roskilde, Denmark, No. 2411, 1983.
- [7] K. Yang, G. Kwak, K. Cho, and J. Huh, "Wind farm layout optimization for wake effect uniformity," *Energy*, vol. 183, pp. 983–995, Sep. 2019, doi: 10.1016/j.energy.2019.07.019.
- [8] G. Marmidis, S. Lazarou, and E. Pyrgioti, "Optimal placement of wind turbines in a wind park using Monte Carlo simulation," *Renewable Energy*, vol. 33, no. 7, pp. 1455–1460, Jul. 2008, doi: 10.1016/j.renene.2007.09.004.
- [9] S. Şişbot, Ö. Turgut, M. Tunç, and Ü. Çamdalı, "Optimal positioning of wind turbines on Gökçeada using multi-objective genetic algorithm," *Wind Energy*, vol. 13, no. 4, pp. 297–306, May 2010, doi: 10.1002/we.339.
- [10] C. Wan, J. Wang, G. Yang, and X. Zhang, "Optimal Micro-siting of Wind Farms by Particle Swarm Optimization," *Advances in Swarm Intelligence: First International Conference, ICSI 2010, Proceedings, Part I 1*, Beijing, China, 2010, pp. 198–205, doi: 10.1007/978-3-642-13495-1_25.
- [11] A. Kusiak and Z. Song, "Design of wind farm layout for maximum wind energy capture," *Renewable Energy*, vol. 35, no. 3, pp. 685–694, Mar. 2010, doi: 10.1016/j.renene.2009.08.019.
- [12] B. Saavedra-Moreno, S. Salcedo-Sanz, A. Paniagua-Tineo, L. Prieto, and A. Portilla-Figueras, "Seeding evolutionary algorithms with heuristics for optimal wind turbines positioning in wind farms," *Renewable Energy*, vol. 36, no. 11, pp. 2838–2844, Nov. 2011, doi: 10.1016/j.renene.2011.04.018.
- [13] R. Archer, G. Nates, S. Donovan, and H. Waterer, "Wind Turbine Interference in a Wind Farm Layout Optimization Mixed Integer Linear Programming Model," *Wind Engineering*, vol. 35, no. 2, pp. 165–175, Apr. 2011, doi: 10.1260/0309-524X.35.2.165.

- [14] Y. Wang, Y. Yu, S. Cao, X. Zhang, and S. Gao, "A review of applications of artificial intelligent algorithms in wind farms," *Artificial Intelligence Review*, vol. 53, no. 5, pp. 3447–3500, Jun. 2020, doi: 10.1007/s10462-019-09768-7.
- [15] X. Shang, D. Shen, F.-Y. Wang, and T. R. Nyberg, "A heuristic algorithm for the fabric spreading and cutting problem in apparel factories," *IEEE/CAA Journal of Automatica Sinica*, vol. 6, no. 4, pp. 961–968, Jul. 2019, doi: 10.1109/JAS.2019.1911573.
- [16] A. Song, G. Wu, W. Pedrycz, and L. Wang, "Integrating Variable Reduction Strategy With Evolutionary Algorithms for Solving Nonlinear Equations Systems," *IEEE/CAA Journal of Automatica Sinica*, vol. 9, no. 1, pp. 75–89, Jan. 2022, doi: 10.1109/JAS.2021.1004278.
- [17] C. Lee, H. Hasegawa, and S. Gao, "Complex-Valued Neural Networks: A Comprehensive Survey," *IEEE/CAA Journal of Automatica Sinica*, vol. 9, no. 8, pp. 1406–1426, Aug. 2022, doi: 10.1109/JAS.2022.105743.
- [18] Z. Lei, S. Gao, Z. Zhang, M. Zhou, and J. Cheng, "MO4: A Many-Objective Evolutionary Algorithm for Protein Structure Prediction," *IEEE Transactions on Evolutionary Computation*, vol. 26, no. 3, pp. 417–430, Jun. 2022, doi: 10.1109/TEVC.2021.3095481.
- [19] M. Wagner, J. Day, and F. Neumann, "A fast and effective local search algorithm for optimizing the placement of wind turbines," *Renewable Energy*, vol. 51, pp. 64–70, Mar. 2013, doi: 10.1016/j.renene.2012.09.008.
- [20] D. H. Wolpert and W. G. Macready, "No free lunch theorems for optimization," *IEEE Transactions on Evolutionary Computation*, vol. 1, no. 1, pp. 67–82, Apr. 1997, doi: 10.1109/4235.585893.
- [21] X. Luo, Y. Yuan, S. Chen, N. Zeng, and Z. Wang, "Position-Transitional Particle Swarm Optimization-Incorporated Latent Factor Analysis," *IEEE Transactions on Knowledge and Data Engineering*, vol. 34, no. 8, pp. 3958–3970, Aug. 2022, doi: 10.1109/TKDE.2020.3033324.
- [22] J. Chen, X. Luo, and M. Zhou, "Hierarchical Particle Swarm Optimization-incorporated Latent Factor Analysis for Large-Scale Incomplete Matrices," *IEEE Transactions on Big Data*, vol. 8, no. 6, pp. 1524–1536, 2021, doi: 10.1109/TBDATA.2021.3090905.
- [23] J. Chen, R. Wang, D. Wu, and X. Luo, "A Differential Evolution-Enhanced Position-Transitional Approach to Latent Factor Analysis," *IEEE Transactions on Emerging Topics in Computational Intelligence*, vol. 7, no. 2, pp. 389–401, 2023, doi: 10.1109/TETCI.2022.3186673.
- [24] T. T. Le and D. N. Vo, "Optimal layout for off-shore wind farms using metaheuristic search algorithms," *GMSARN International Journal*, vol. 11, no. 1, pp. 1–15, 2017.
- [25] S. Mirjalili and A. Lewis, "The Whale Optimization Algorithm," *Advances in Engineering Software*, vol. 95, pp. 51–67, May 2016, doi: 10.1016/j.advengsoft.2016.01.008.
- [26] T. Kunakote *et al.*, "Comparative Performance of Twelve Metaheuristics for Wind Farm Layout Optimisation," *Archives of Computational Methods in Engineering*, vol. 29, no. 1, pp. 717–730, Jan. 2022, doi: 10.1007/s11831-021-09586-7.
- [27] M. Beşkiri, I. Koç, H. Haki, and H. Kodaz, "A new optimization algorithm for solving wind turbine placement problem: Binary artificial algae algorithm," *Renewable Energy*, vol. 121, pp. 301–308, Jun. 2018, doi: 10.1016/j.renene.2017.12.087.
- [28] Y. Eroglu and S. U. Seçkiner, "Design of wind farm layout using ant colony algorithm," *Renewable Energy*, vol. 44, pp. 53–62, Aug. 2012, doi: 10.1016/j.renene.2011.12.013.
- [29] H. Hakli, "BinEHO: a new binary variant based on elephant herding optimization algorithm," *Neural Computing and Applications*, vol. 32, no. 22, pp. 16971–16991, Nov. 2020, doi: 10.1007/s00521-020-04917-4.
- [30] A. C. Pillai, J. Chick, L. Johanning, and M. Khorasanchi, "Offshore wind farm layout optimization using particle swarm optimization," *Journal of Ocean Engineering and Marine Energy*, vol. 4, no. 1, pp. 73–88, Feb. 2018, doi: 10.1007/s40722-018-0108-z.
- [31] H. Long, P. Li, and W. Gu, "A data-driven evolutionary algorithm for wind farm layout optimization," *Energy*, vol. 208, p. 118310, Oct. 2020, doi: 10.1016/j.energy.2020.118310.
- [32] X. Ju, F. Liu, L. Wang, and W.-J. Lee, "Wind farm layout optimization based on support vector regression guided genetic algorithm with consideration of participation among landowners," *Energy Conversion and Management*, vol. 196, pp. 1267–1281, Sep. 2019, doi: 10.1016/j.enconman.2019.06.082.
- [33] F. Bai, X. Ju, S. Wang, W. Zhou, and F. Liu, "Wind farm layout optimization using adaptive evolutionary algorithm with Monte Carlo Tree Search reinforcement learning," *Energy Conversion and Management*, vol. 252, p. 115047, Jan. 2022, doi: 10.1016/j.enconman.2021.115047.
- [34] S. Saremi, S. Mirjalili, and A. Lewis, "Grasshopper Optimisation Algorithm: Theory and application," *Advances in Engineering Software*, vol. 105, pp. 30–47, Mar. 2017, doi: 10.1016/j.advengsoft.2017.01.004.
- [35] Y. Meraihi, A. B. Gabis, S. Mirjalili, and A. Ramdane-Cherif, "Grasshopper Optimization Algorithm: Theory, Variants, and Applications," *IEEE Access*, vol. 9, pp. 50001–50024, 2021, doi: 10.1109/ACCESS.2021.3067597.
- [36] Z. Elmi and M. O. Efe, "Multi-objective grasshopper optimization algorithm for robot path planning in static environments," in *2018 IEEE International Conference on Industrial Technology (ICIT)*, Feb. 2018, pp. 244–249, doi: 10.1109/ICIT.2018.8352184.
- [37] M. Abdulrahman and D. Wood, "Wind Farm Layout Upgrade Optimization," *Energies*, vol. 12, no. 13, p. 2465, Jun. 2019, doi: 10.3390/en12132465.
- [38] "WASP software." www.wasp.dk, (accessed May 2024).
- [39] "windPRO software." <http://www.emd.dk/windpro>, (accessed May 2024).
- [40] K. A. Singh, M. G. M. Khan, and M. R. Ahmed, "Wind Energy Resource Assessment for Cook Islands With Accurate Estimation of Weibull Parameters Using Frequentist and Bayesian Methods," *IEEE Access*, vol. 10, pp. 25935–25953, 2022, doi: 10.1109/ACCESS.2022.3156933.
- [41] R. Dhakal, A. Sedai, S. Pol, S. Parameswaran, A. Nejat, and H. Moussa, "A Novel Hybrid Method for Short-Term Wind Speed Prediction Based on Wind Probability Distribution Function and Machine Learning Models," *Applied Sciences*, vol. 12, no. 18, p. 9038, Sep. 2022, doi: 10.3390/app12189038.
- [42] H. R. Alsamamra, S. Salah, J. A. H. Shoqir, and A. J. Manasra, "A comparative study of five numerical methods for the estimation of Weibull parameters for wind energy evaluation at Eastern Jerusalem, Palestine," *Energy Reports*, vol. 8, pp. 4801–4810, Nov. 2022, doi: 10.1016/j.egy.2022.03.180.
- [43] I. Okakwu, D. Akinyele, O. Olabode, T. Ajewole, E. Oluwasogo, and A. Oyediji, "Comparative Assessment of Numerical Techniques for Weibull Parameters' Estimation and the Performance of Wind Energy Conversion Systems in Nigeria," *IJUM Engineering Journal*, vol. 24, no. 1, pp. 138–157, Jan. 2023, doi: 10.31436/ijumej.v24i1.2611.
- [44] R. Shakoor, M. Y. Hassan, A. Raheem, and Y.-K. Wu, "Wake effect modeling: A review of wind farm layout optimization using Jensen's model," *Renewable and Sustainable Energy Reviews*, vol. 58, pp. 1048–1059, May 2016, doi: 10.1016/j.rser.2015.12.229.
- [45] C. L. Archer *et al.*, "Review and evaluation of wake loss models for wind energy applications," *Applied Energy*, vol. 226, pp.




- 1187–1207, Sep. 2018, doi: 10.1016/j.apenergy.2018.05.085.
- [46] T. Göçmen, P. van der Laan, P.-E. Réthoré, A. P. Diaz, G. C. Larsen, and S. Ott, “Wind turbine wake models developed at the technical university of Denmark: A review,” *Renewable and Sustainable Energy Reviews*, vol. 60, pp. 752–769, Jul. 2016, doi: 10.1016/j.rser.2016.01.113.
- [47] N. Kermani, S. Andersen, J. Sørensen, and J. N. Shen, “Analysis of turbulent wake behind a wind turbine,” *International Conference on aerodynamics of Offshore Wind Energy Systems and wakes (ICOWES 2013)*, 2013, no. June, pp. 53–68.
- [48] M. Bastankhah and F. Porté-Agel, “A new analytical model for wind-turbine wakes,” *Renewable Energy*, vol. 70, pp. 116–123, Oct. 2014, doi: 10.1016/j.renene.2014.01.002.
- [49] L. Niemeyer, L. Pietronero, and H. J. Wiesmann, “Fractal Dimension of Dielectric Breakdown,” *Physical Review Letters*, vol. 52, no. 12, pp. 1033–1036, Mar. 1984, doi: 10.1103/PhysRevLett.52.1033.
- [50] M. S. M. Raj, M. Alexander, and M. Lydia, “Modeling of wind turbine power curve,” in *ISGT2011-India*, Dec. 2011, pp. 144–148, doi: 10.1109/ISGT-India.2011.6145371.
- [51] I. Hussain, A. Haider, Z. Ullah, M. Russo, G. M. Casolino, and B. Azeem, “Comparative Analysis of Eight Numerical Methods Using Weibull Distribution to Estimate Wind Power Density for Coastal Areas in Pakistan,” *Energies*, vol. 16, no. 3, p. 1515, Feb. 2023, doi: 10.3390/en16031515.

BIOGRAPHIES OF AUTHORS






Khoa Dang Nguyen    was born in Long An Province, Vietnam. He received his B.Eng. degree in Electrical Engineering and M.Eng. degree in Electric Equipment, Network and Machine from Ho Chi Minh City University of Technology, VNU-HCM in 2002 and 2013, respectively. He is working at Faculty of Electrical Engineering, College of Engineering, Can Tho University. He is currently working toward the Ph.D. degree at Department of Power Systems, Faculty of Electrical and Electronic Engineering, Ho Chi Minh City University of Technology. His research interests are power system optimization and renewable energy integrated in power systems. He can be contacted at email: nguyendangkhoa.sdh21@hcmut.edu.vn.



Tinh Trung Tran    was born in Long An Province, Vietnam. He received B.Sc. from Can Tho University in 1997; M.Sc. and Ph.D. degrees from Gyeongsang National University in 2004 and 2007 respectively. His research interest includes power system expansion planning, fuzzy set theory applications and reliability evaluation of power systems. Since 1997, he has been on the College of Engineering–Can Tho University where he is now an Assoc. Professor. He can be contacted at email: ttinh@ctu.edu.vn.



Dieu Ngoc Vo    was born in Dong Thap Province, Vietnam. He received his B.Eng. and M.Eng. degrees in Electrical Engineering from Ho Chi Minh City University of Technology (HCMUT), VNU-HCM, Ho Chi Minh City, Vietnam, in 1995 and 2000, respectively and his D.Eng. degree in Energy from Asian Institute of Technology (AIT), Pathumthani, Thailand in 2007. He is currently a lecturer at Department of Power Systems, Faculty of Electrical and Electronic Engineering, HCMUT. His interests are applications of AI in power system optimization, power system operation and control, power system analysis, and power systems under deregulation. He can be contacted at email: vndieu@hcmut.edu.vn.